The Journal of the Korean Society of
Coastal and Ocean Engineers
Vol. 4, No. 1, pp. 45~58, March 1992

Computation of Meteorologically-Induced Circulation on the East China Sea using a Fine Grid Three-dimensional Numerical Model
細格子三次元 數値 模型에 의한 東中國海의 氣象學的으로 誘發된 海流循環의 算定

Byung Ho Choi* and Kyung Suk Suh**
崔秉昊* · 徐景錫**

Abstract □ A three-dimensional hydrodynamic numerical model is used to compute the annual and seasonal• meteorologically-induced residual circulation on the Yellow Sea and the East China Sea continental shelf. The model is formulated having irregular coastal boundaires and non-uniform depth distribution representative of nature. The previous three-dimensional model of the East China Sea (Choi, 1984) has been further refined to resolve the flow over the continental shelf in more detail. The mesh resolution of the present finite difference grid system used is 4 minutes latitude by 5 minutes longitude over the entire shelf. The circulation pattern showing depth and spatial distribution of currents over the Yellow Sea and the East China Sea is presented. Meteorologically-induced currents are subsequently used to compute turn-over times for the three depths (surface, mid-depth, bottom) and the total water column of various regions of the Yellow Sea and the East China Sea.

要 旨 : 黃海 및 東中國海에서 氣象學的으로 誘發된 年平均 및 季節的 海流 循環을 算定하기 위해 3次元 數値模型이 이용되었는데 數値模型은 불규칙한 沿岸境界와 실제 水深을 反映할 수 있도록 構成되었다. 본 硏究에서는 前回의 東中國海의 3차원 數値模型 (Choi, 1984)을 陸棚域에서의 흐름을 좀더 자세히 再現할 수 있도록 細分化하였는데 模型에 사용된 有限格子體系의 海像度는 緯度 4分과 經度 5分으로 構成되었으며 黃海 및 東中國海上에서 流速의 3次元的 循環 形態가 算定되어 提示되었다. 數値模型에 의해 계산된 氣象學的으로 誘發된 恒流 流速은 이 海域의 여러 領域에서 水深(표면, 중간수심, 바닥)別 및 전체 水柱에 대해 海水 交滯時間을 계산하는데 利用되었다.

1. INTRODUCTION

In the previous studies (Choi, 1982, 1984) wind-induced currents in the East China Sea under steady uniform wind stress conditions were derived from two-dimensional and three-dimensional numerical model. Those model had a grid resolution with 1/5° latitude by 1/4° longitude over the entire shelf. The results of the above work were only able to describe the response of the shelf to stationary wind stress fields suddenly imposed on the Yellow Sea and the East China Sea shelf. Subsequently, numerical experiments using a three-dimensional model (grid resolution 1/5° latitude by 1/4° longitude) with more physically realistic averaged wind fields had been performed to examine the spatial distribution of annual and seasonal meteorogically induced residual circulation on the shelf (Choi and Suh, 1991).

With the advent of expanding computer power and increasing necessity of resolving the flow with enough details, the previous model (Choi, 1984) has been further improved to higher resolution of 1/15° latitude by 1/12° longitude covering the entire continental shelf and investigated the spatial distribution of annual and seasonal meteorologically induced residual circulation in more detail. A staggered finite difference scheme is presented in horizontal as

*成均館大學校 土木工學科(Department of Civil Engineering, Sung Kyun Kwan University, Suwon 170, Korea)
**韓國原子力硏究所(Korea Atomic Energy Research Institute, P.O. Box 7, Daeduk-Danji, Daejeon, Korea)

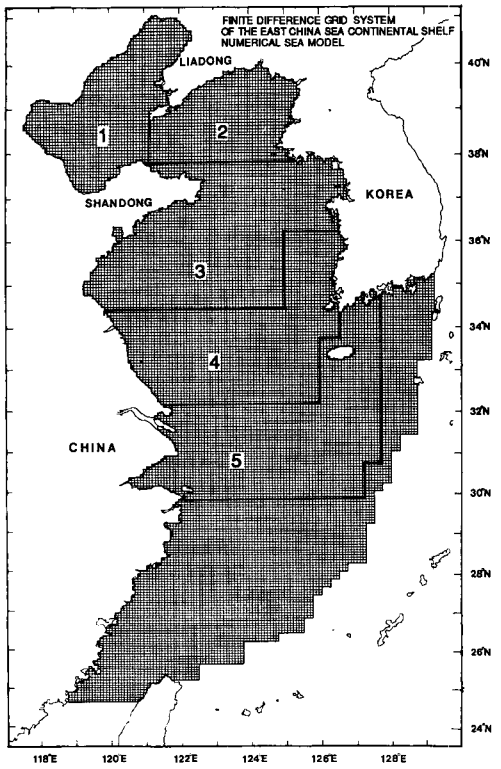

Fig. 1. Finite difference grid of the model, and divided sea regions used to compute turn-over times.

shown in Fig. 1. Meteorological effects coupled with variation in the bottom topography are important factors which determine the residual circulation. Also, meteorologically-induced currents in shallow sea areas exhibit considerable vertical shear, giving rise to significant differences in current magnitude and direction through the vertical, neccessitating the use of a full three-dimensional model.

Recently, Choi(1989) has successfully used a fine mesh three-dimensional hydrodynamic model with the same grid resolution of present study to reproduce the three-dimensional current structure of the M_2 tide representing the dominant tidal conditions of the East China Sea continental shelf. The hydrodynamic equations used in the model are linear with the exception of a quadratic bottom friction and the solutions are obtained by Galerkin method using a basis set of cosine functions. Among the some parameters used in the model, we consider the special case in which the vertical eddy viscosity is independent of the depth coordinates and a quadratic law of bottom friction at the sea bed is employed. Along the open boundaries of the model, a radiation condition is employed to allow disturbances from the interior of the model to propagate outwards. The numerical techniques are based on modelling by Heaps(1972) and Davies(1980).

In this paper annual and seasonal wind stress and pressure data based on observations (Han and Lee, 1981; JMA, 1968) are used to calculate the meteorologically-induced residual currents on the shelf. The computed spatial distribution of currents at three depths from season to season are presented. The model assumes that the sea is homogeneous, which is physically realistic over most of the shelf during the winter periods but not during the summer months when regions of the shelf are stratified.

These meteorologically-induced currents are then used to compute turn-over times for various divided regions of the Yellow Sea and East China Sea. Also, the computed turn-over times with present model is compared with those by the coarse grid model (Choi and Suh, 1991) and discussed.

2. HYDRODYNAMIC EQUATIONS

The equations of continuity and motion for homogeneous water neglecting non-linear terms, shear in the horizontal and the direct influence of the tide-generating potentials, may be written in spherical polar coordinates as

$$\frac{\partial \xi}{\partial t}+\frac{1}{R\cos\phi}\left(\frac{\partial}{\partial \chi}\int_0^h u\,dz+\frac{\partial}{\partial \phi}\int_0^h v\cos\phi dz\right)=0 \quad (1)$$

$$\frac{\partial u}{\partial t}-\gamma v=-\frac{g}{R\cos\phi}\frac{\partial \xi}{\partial \chi}-\frac{1}{\rho R\cos\phi}\frac{\partial P}{\partial \chi}+\frac{\partial}{\partial z}\left(N\frac{\partial u}{\partial z}\right) \quad (2)$$

$$\frac{\partial v}{\partial t}+\gamma u=-\frac{g}{R}\frac{\partial \xi}{\partial \phi}-\frac{1}{\rho R}\frac{\partial P}{\partial \phi}+\frac{\partial}{\partial z}\left(N\frac{\partial v}{\partial z}\right) \quad (3)$$

where

χ, ϕ: east-longitude and north-latidude, respectively

z : depth below the undisturbed surface

t : time
ξ : elevation of the sea surface above the undisturbed level
h : undisturbed depth of water
ρ : the density of sea water
P : atmospheric pressure at the sea surface
R : the radius of the earth
γ : Coriolis parameter ($\gamma\omega\sin\phi$)
ω : angular speed of the Earth's rotation
g : the acceleration due to gravity
u, v : the east-going and north-going components of current at depth z
N : coefficient of vertical eddy viscosity

In oder to solve Eqs. (1), (2) and (3) for ξ, u and v, the appropriate boundary conditions at the sea surface and sea bed have to be specified. The surface conditions are:

$$-\rho\left(N\frac{\partial u}{\partial z}\right)_o = F_S, \quad -\rho\left(N\frac{\partial v}{\partial z}\right)_o = G_S \qquad (4a, b)$$

where Fs, Gs donote the components of wind stress acting on the sea surface in the χ and ϕ direction, subscript zero denoting evaluation at z=0.

Assuming a slip boundary condition at the sea bed (z=h) and using a quadratic law of bottom friction yeils,

$$-\rho\left(N\frac{\partial u}{\partial z}\right)_h = k\rho u_h\sqrt{u_h^2+v_h^2} \qquad (5a)$$

$$-\rho\left(N\frac{\partial v}{\partial z}\right)_h = k\rho v_h\sqrt{u_h^2+v_h^2} \qquad (5b)$$

where k is the coefficient of quadratic bottom friction, taken as constant.

By expanding the two components of velocity u, v in terms of depth-dependent functions (basis functions) and horizontal-space and time dependent coefficients, Eqs. (1), (2) and (3) can be solved using the Galerkin method in vertical and finite difference grid in horizontal.

For the choice of basis functions, Davies and Furnes (1980) have shown that an expansion of only 10 cosine functions is sufficient to accurately reproduce the depth variation of current. Choi (1985) also has applied such an expansion to the computation of the M_2, S_2, K_1 and O_1 tides of the East China Sea continental shelf in previous model. A full description of Galerkin method is given in Davies (1980) and will not be restated here.

The particular case in which the vertical eddy viscosity N is independent of depth coordinate z is considered. Along a closed boundary the normal component of current is set to zero, for all t≥0. Along the open boundaries of the model, a radiation condition is employed to allow disturbances from the interior of the model to pass outward. This condition involves a prescribed relation between the total normal component of depth-mean current q and total elevation ξ given by:

$$q=\frac{c}{h}(\xi-\xi_M) \qquad (6)$$

where $c=\sqrt{gh}$ and the meterorologically induced sea surface elevation ξ_M, is determined from

$$\xi_M(\chi,\phi,t)=\frac{\bar{P}-P(\chi,\phi,t)}{\rho g} \qquad (7)$$

where $\bar{P}$ is a mean atmospheric pressure taken to be 1012 mbar, and $P(\chi,\phi,t)$ is the atmospheric pressure at the sea surface at point χ, ϕ on the model's open boundary at time t.

3. TURN-OVER TIME

The concept of a turn-over time for a sea area is particularly important in understanding pollution problems. Consider various divided regions of the sea area, and assume that this divided region is in exchange with other regions. Then the turn-over time T is ususally expressed as the ratio of the total mass in the sea area to the total flux (Bolin and Rodhe, 1973).

$$T=M/F \qquad (8)$$

where M is the total mass of water in the divided sea area, and F is the total flux of mass leaving per unit time. Since density is constant in the model, mass is replaced by volume, and mass flux by volume flux in the above Eqs. (8).

$$T=V/q \qquad (9)$$

where V is the total volume of water in the divided

sea area, and q is th total volume flux though the boundaries of divided sea area. In the steady state, when the total mass, fluxes and internal processes within a sea area are independent of time, the turn-over time, is equivalent to the residence time or average transit time, and is the mean time water particles have been in the sea area at the moment they are leaving it (Bolin and Rodhe, 1973). With the finite difference grid of the Yellow Sea and the East China Sea, surface elevation (ξ), is computed at the centre of the grid square, the north-south component of current (v), at the northern and southern sides of the square, and the west-east component of current (u), at the western and eastern sides. Using such grid, the flux through a divided area can be readily computed, provided the boundaries of the area coincide with the grid lines used in the model. In order to compute turn-over time of each block, the East China Sea continental shelf is divided into five region as is seen in Fig. 1. This region is divided in arbitrarily manner, which is the same divided blocks to the previous model (Choi and Suh, 1991).

4. COMPUTED METEOROLOGICALLY INDUCED RESIDUAL CURRENTS AND TURN-OVER TIMES

4.1 Meteorologically induced residual currents

As shown in Fig. 1 the grid spacing of the present model is about 4 nautical miles resulting from one third refinement of the grid system in the previous coarse shelf model (Choi, 1980). The total number of grid points is over 35,000 and 60% of total grids are practical computation points. The time step for stable difference solutions according to the Courant-Friedrichs-Lewy criterion was chosen as 69.003s. The computations covered the period of real time from t=0 to t=60 hours with physically realistic averaged wind fields and pressure data. The coefficient of bottom friction (k) and vertical eddy viscosity (N) used a value of 0.002 m/sec and 0.065 m^2 /sec uniformly over the region, respectively.

The seasonal wind stress distributions over the shelf for four seasons, December/January/February, March/April/May, June/July/August, September/October/November and the annual mean wind stress at grid points of the model as shown in Fig. 2 were interpolated from the 5 degrees by 5 degrees observed wind stress distributions published by Han and Lee (1981). Annual and seasonal atmospheric pressure gradients over the shelf, and the distributions of sea level pressure along the model's open boundaries for use in Eqs. (7) were interpolated from published data by JMA (1968).

In order to determine the meteorologically induced circulation on the shelf, five separate runs were performed, four runs for four seasons and one run using annual mean meteorological input. Fig. 3 to 6 show the meteorologically induced currents at three depths (surface, mid-depth, and bottom) on the shelf for four seasons and the results are similar to the previous coarse shelf model, but providing more detailed circulation pattern.

It is seen from Fig. 3 to 6 that the surface currents for winter, spring and autumn exhibit a outstanding southwest going flow of water through the Taiwan Strait, induced by the predominant northeasterly wind stresses. Also, the surface currents in these seasons are occured to westsouthly going flow of water in the left side of Jeju island. In contrast the surface current during the summer exhibits a northeast going flow through the Taiwan Strait induced by southwesterly wind streses. Also, in this summer season the current flows down southeastly from 33° N to about 38°N in the right side of mid- Yellow Sea. A small counter clockwise gyre in the middle of the East China Sea and a clockwise gyre in the lower position of Jeju island is shown. The stong water flows down along the Chinese coast and subsequently leaves the East China Sea though the Taiwan Starit. Despite the changes in magnitude and direction only during the summer, these major features of the East China Sea circulation persist throughout the winter, spring and autumn seasons.

Currents at the mid-depths for the winter, spring and autumn seasons exhibit large scale counter clockwise reversal of current from 33°N to about 37°N in the Yellow Sea off mid-Chinese coast, a smaller counter clockwise gyre in the Pohai Strait and clockwise gyres at Seohan Bay and off Taean peninsula along the Korean coast despite the changes in mag-

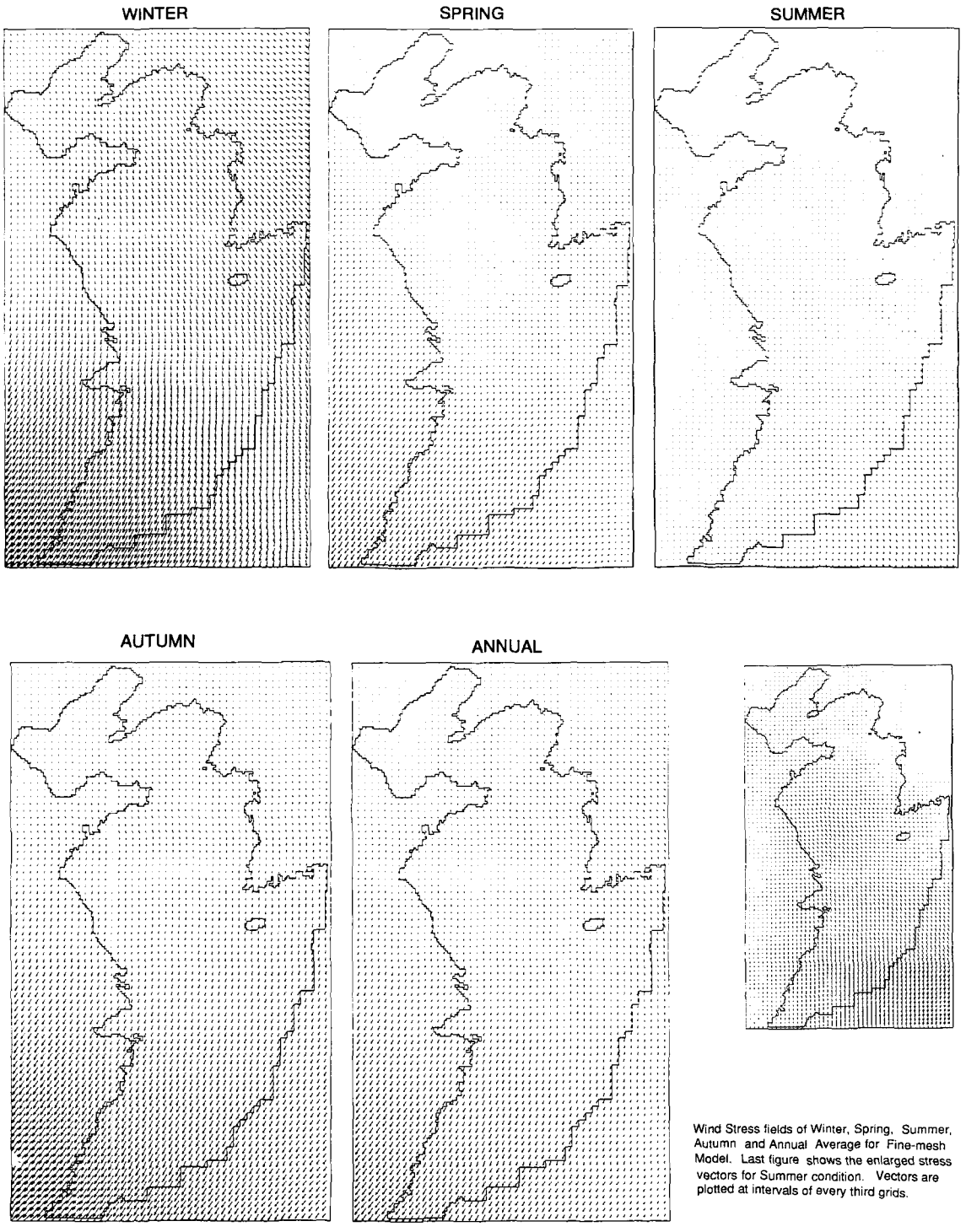

Fig. 2. Wind stress fields of Winter, Spring, Summer, Autumn and annual average. Last figure shows the enlarged vectors for summer condition.

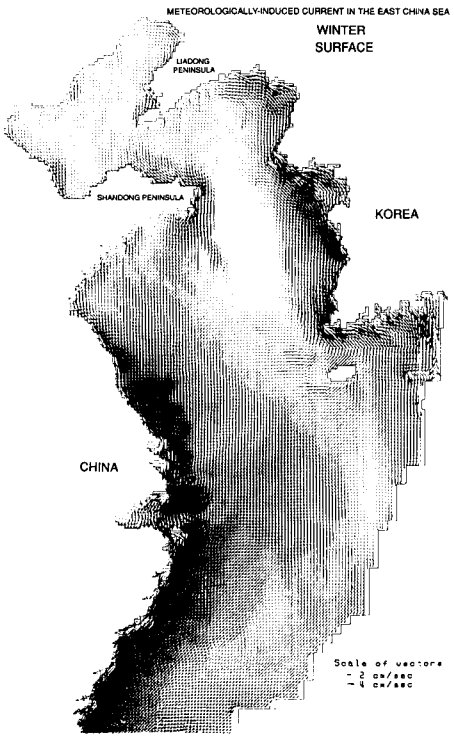

(a)

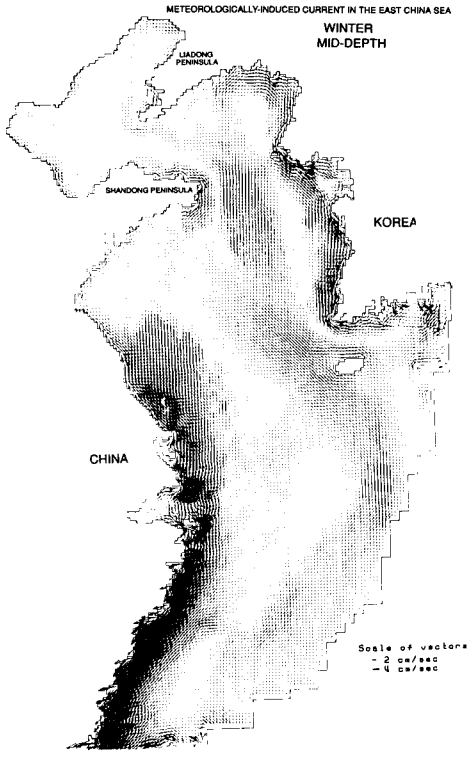

(b)

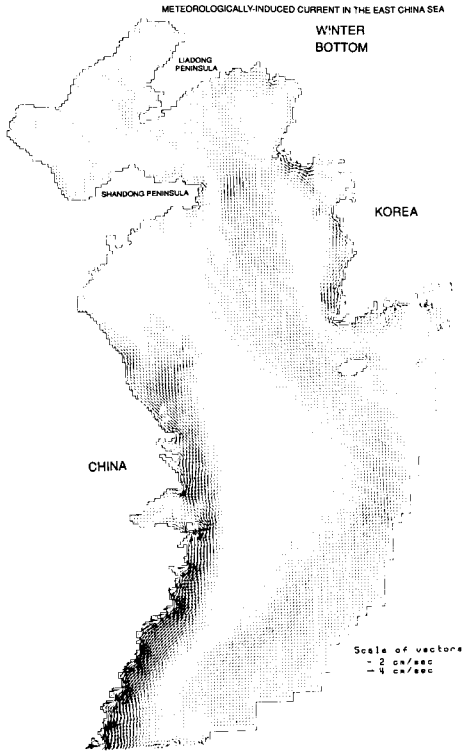

(c)

Fig. 3. Meteorologically-induced currents for period December-February.
3(a) surface current, 3(b) mid-depth current, 3(c) bottom current

nitude of currents. A circulation pattern for the Yellow Sea corresponding this large scale counter clockwise rotation of currents for the winter season has been postulated by Niino and Emery (1961) and by U.S. Naval Oceanographic Office (1964). Other noticeable features of mid-depth circulation during these seasons are north going flow in the middle of the Yellow Sea and northwest going flow in the left of Jeju island.

In the summer current at mid-depth shows an northwest influx of water through the Taiwan Strait and at approximately the latitude of 27°N this water mass bifurcates, with some waters flowing due northwards along the Chinese coast, and southeastly flow down in the middle of the Yellow Sea and near the Jeju island. The spatial distribution of bottom currents in the Yellow sea and the East China Sea from season to season also show similar domi-

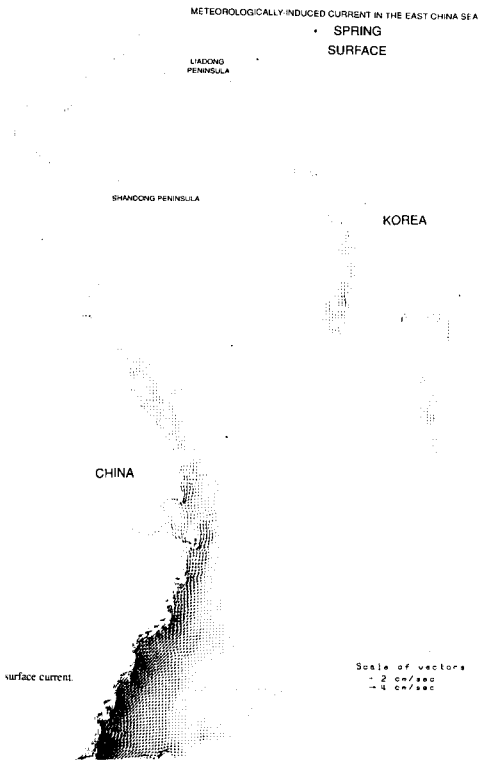

(a)

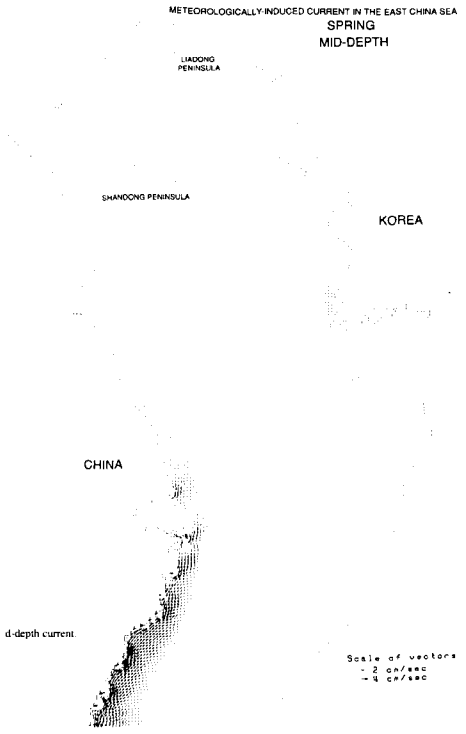

(b)

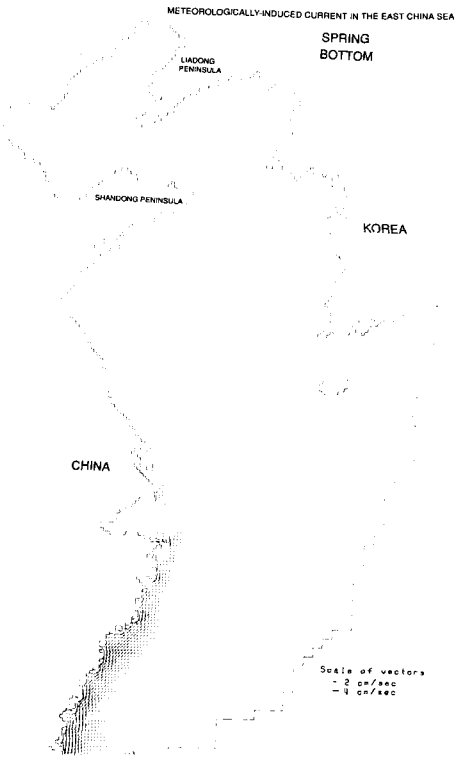

(c)

Fig. 4. Meteorologically-induced currents for period March-May.
4(a) surface current, 4(b) mid-depth current, 4(c) bottom current

nant features of circulation to mid-depths. The spatial variation of bottom current is high presumably due to the influence of bottom topography.

The currents induced by the annual mean wind stress and pressure gradients are shown in Fig. 7. In the figure the dominant south going coastal current along the Chinese coast and the Korean coast are shown at the surface. In particular a counter clockwise gyre in the offshore of mid Chinese coast, clockwise gyres in Seohan Bay, off Taean Peninsula and west going flow in the Jeju Strait are also shown at the mid-depth and bottom. In general the changes in magnitude and direction of currents from season to season are noticeable and the meteorologically induced currents in the East China Sea are stronger than those of the Yellow Sea.

4.2 Calculation of turn-over time

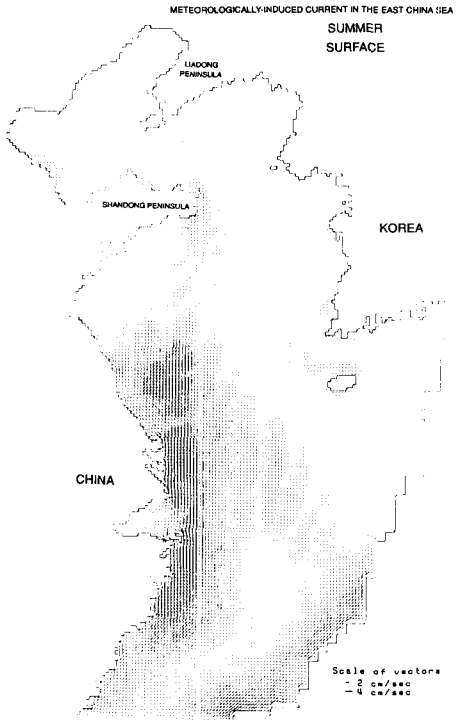

(a)

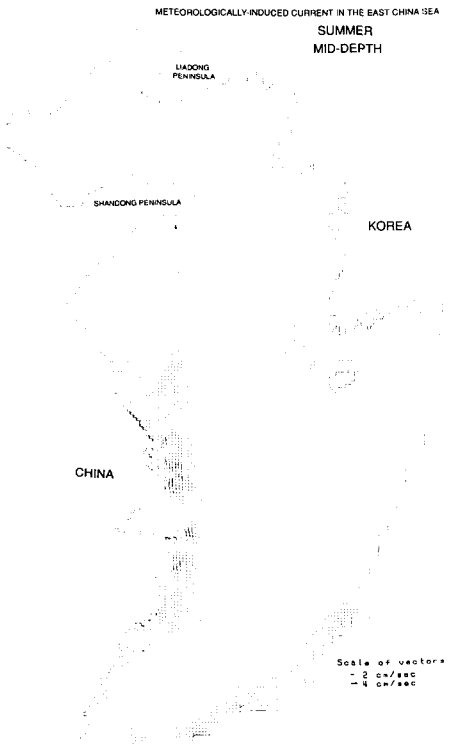

(b)

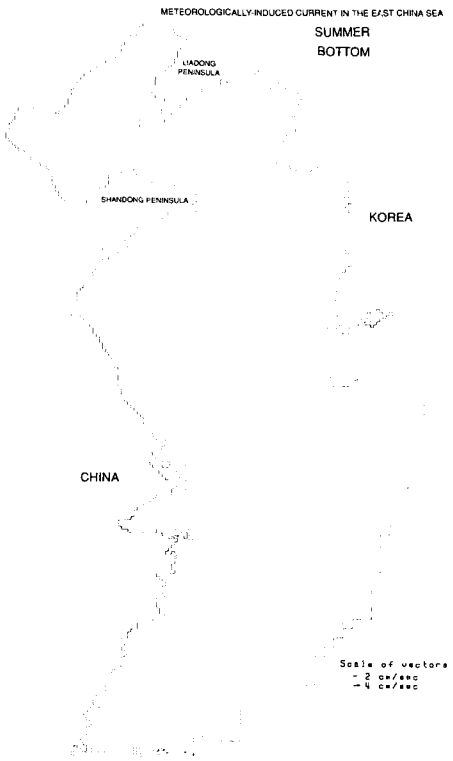

(c)

Fig. 5. Meteorologically-induced currents for period June-August.
5(a) surface current, 5(b) mid-depth current, 5(c) bottom current

Since the magnitude of the meterorologically induced currents from season to season are different, the values of turn-over time for the divided the East China Sea will have a seasonal variation. The magnitude of current also changes through depth, and this variation will be considered the calculation of turn-over time.

For each divided region of the East China Sea (Fig. 1), for the respective seasonal and annual circulations, turn-over times were calculated for the surface, mid-depth and bottom layer, and for the entire water column from sea surface to sea bed. The turn-over time for each block can be readily computed once the volume of the block and the flux through it, are known. In the numerical model the surface area and averaged depth of each grid box are known exactly. Hence the total volume and surface area for each divided sea region can be

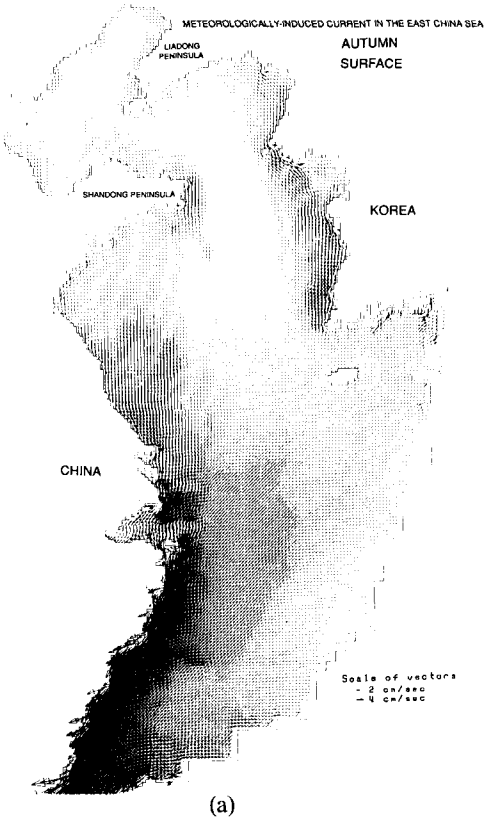

(a)

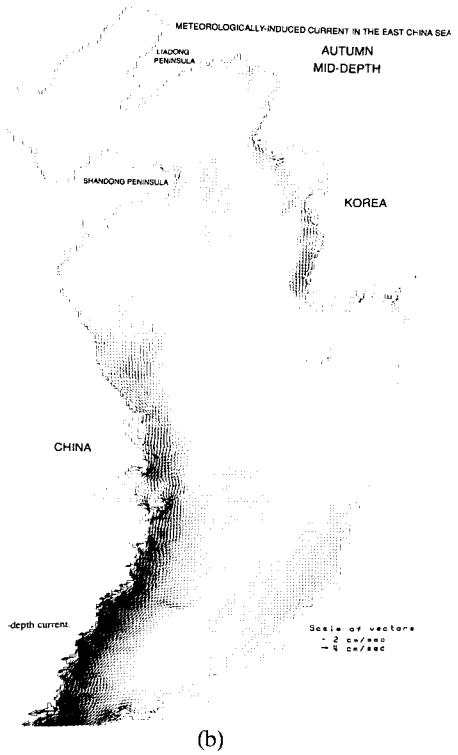

(b)

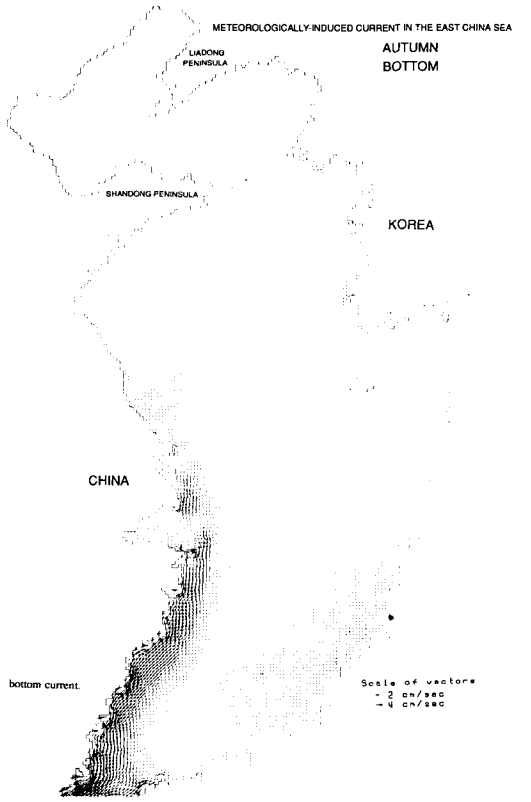

(c)

Fig. 6. Meteorologically-induced currents for period September-November.
6(a) surface current, 6(b) mid-depth current, 6(c) bottom current

determined (Table 1).

The changes in current direction from sea surface to sea bed do occur over most of the East China Sea except the coastal regions. It is therefore necessary to determine at each grid point, the positions within the water column, at which the current reverses, and to compute separately the influx and the outflux of the column. Since the numerical model calculates currents across each side of a grid box, the influx and outflux of each block can be readily computed provided the boundaries of the block coincide with the grid lines used in the three-dimensional numerical shelf model. Having determined the flux into and the flux out of the block, at each grid point on the boundary of the block, the total flux into and flux out of the block can be computed separately summing the individual fluxes. Using this

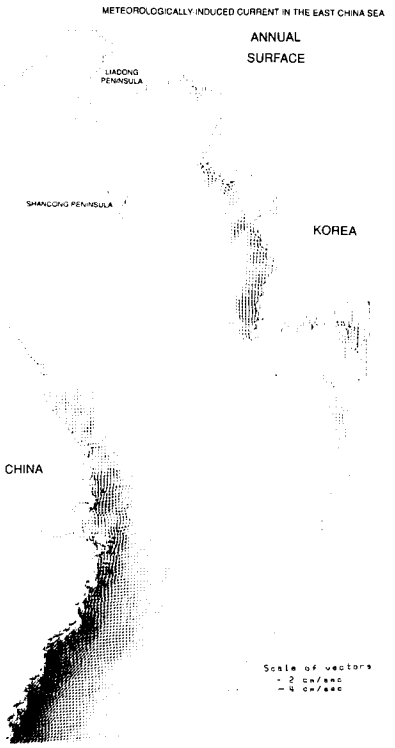

(a)

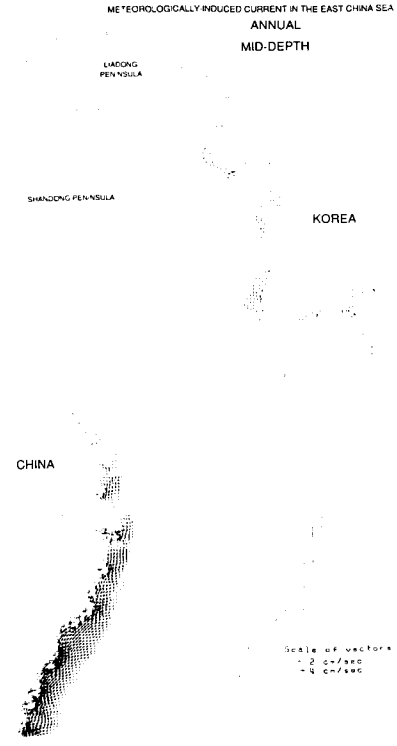

(b)

(c)

Fig. 7. Meteorologically-induced currents for an annual period.
7(a) surface current, 7(b) mid-depth current, 7(c) bottom current

Table 1. Volumes and surface areas of each divided region in the East China Sea.

Divided region	Total volume(m^3)	Surface area(m^2)
1	1.64×10^{12}	5.5×10^{11}
2	2.71×10^{12}	9.0×10^{11}
3	8.77×10^{12}	3.0×10^{12}
4	6.86×10^{12}	2.2×10^{12}
5	1.10×10^{13}	3.6×10^{12}

method the flux in or out over the boundaries of each divided region of the East China Sea was computed and the turn-over time was determined from Eqs. (9), by the volumes given Table 1, by the corresponding volume flux through it. The turn-over time for the three layer can be computed the volume of each layer dividing by the total volum flux through the layer.

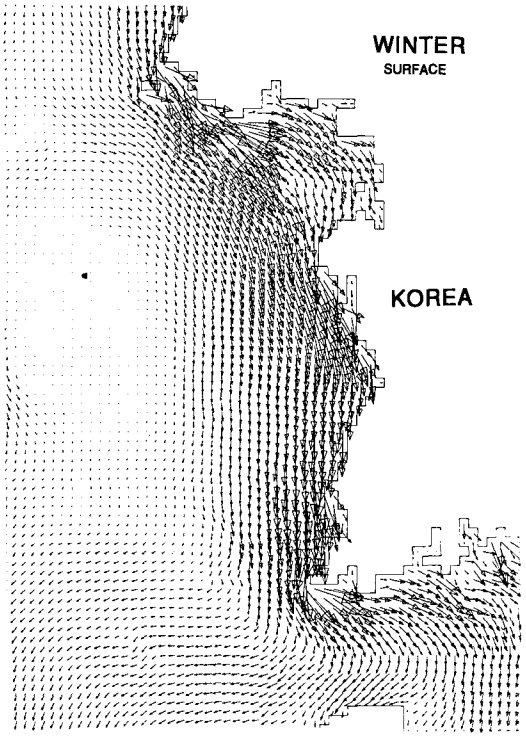

(a)

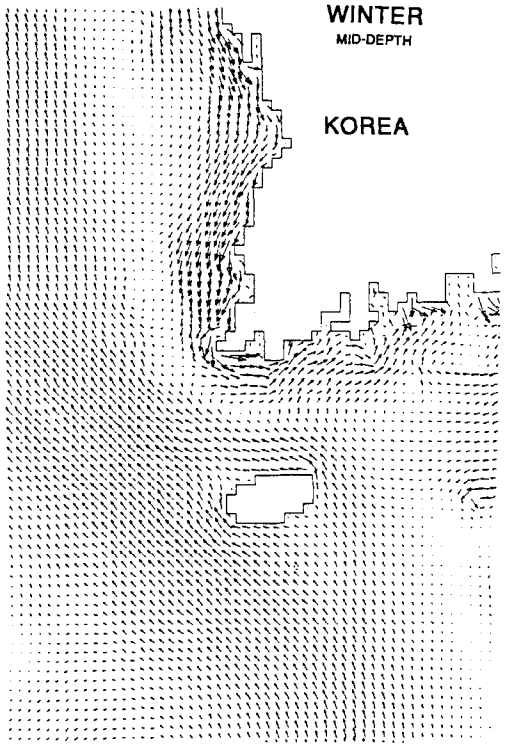

(b)

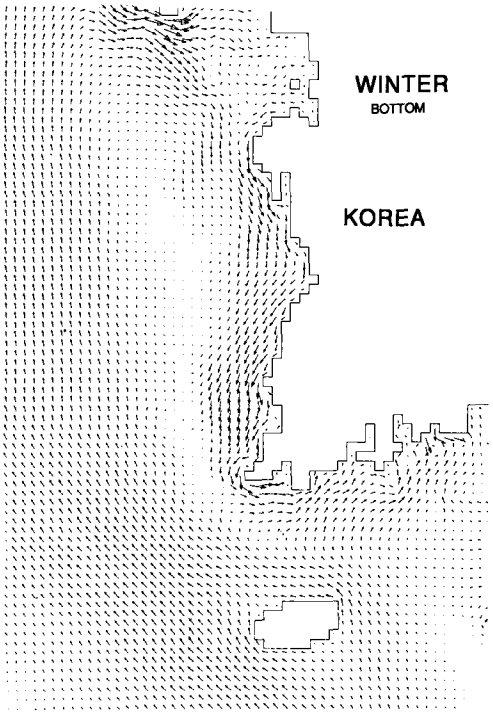

(c)

Fig. 8. Blow up of Fig(3) for the west coast of Korea, Eastern Yellow Sea, for winter circulation.
8(a) surface current, 8(b) mid-depth current, 8(c) bottom current

Table 2. Turn-over time (years) computed with meteorological forcing averaged over a year

Divided region	Surface layer	Mid-depth layer	Bottom layer	3D
1	7.7	7.8	15.9	9.4
2	0.8	2.9	8.4	1.8
3	1.4	2.8	4.3	2.3
4	0.9	1.6	2.6	1.4
5	0.7	2.0	2.5	1.2

Computed the turn-over time using annual meteorologically-induced current is presented Table 2. In this table the column headed "3D" gives the turn-over time taking into account changes in current direction through the water column. Since the turn-over time using depth-mean current from Eqs. (9) has a smilar with that of mid-depth layer in the three-dimensional numerical model, the turn-over time in mid-depth layer is regarded as it in

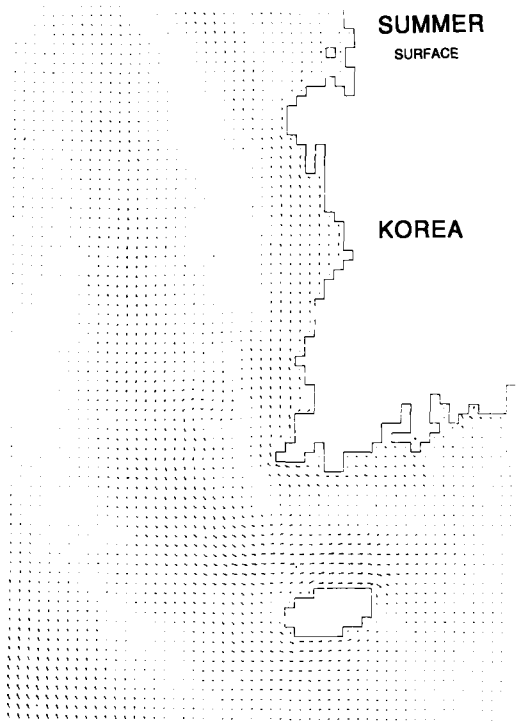

(a)

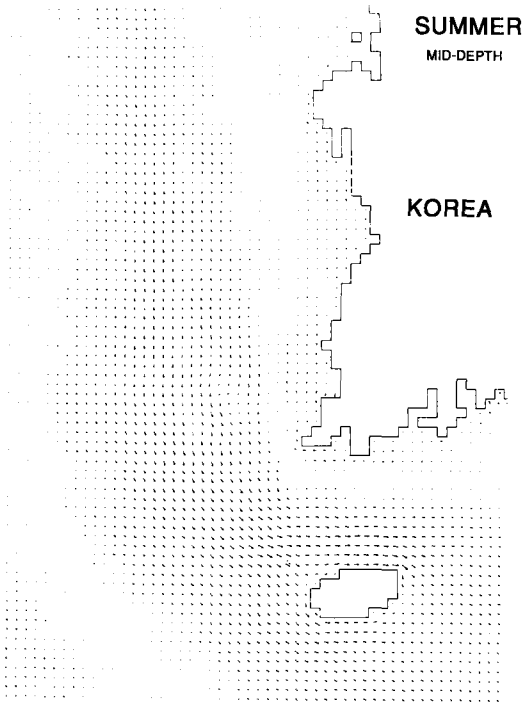

(b)

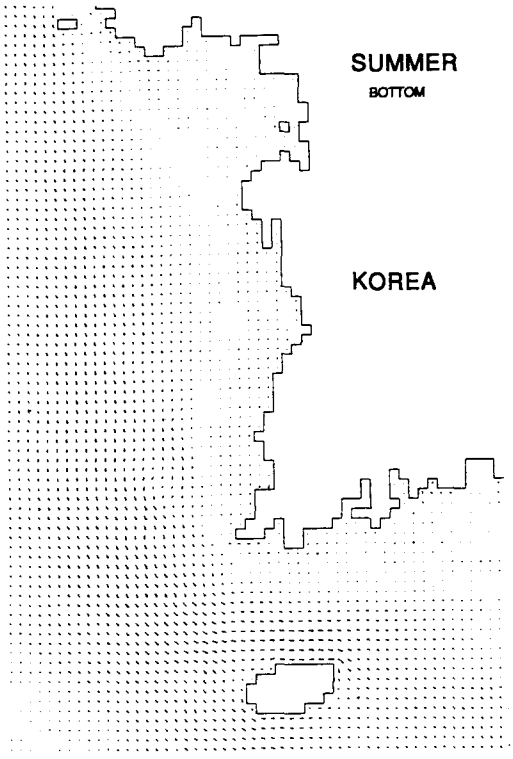

(c)

Fig. 9. Blow up of Fig(5) for the west coast of Korea, Eastern Yellow Sea, for winter circulation.
9(a) surface current, 9(b) mid-depth current, 9(c) bottom current

2D.

It is apparent from a comparison of these two values that the "3D" turn-over time is significantly lower than the 2D except block 1. This difference is that a two-dimensional numerical model would compute only a depth-mean current, whereas a three-dimensional numerical model would take into account to change in current direction through the water column. So the turn-over time associated with 2D may be unrealistically long. But the turn-over time in 3D is higher than that of 2D in block 1. For this reason is presumed with the following two facts. First, since the configuration of block 1 as is seen in Fig. 1 is composed of closed boundary except one sea boundary, the flux is exchanged through it. Therefore the flux into this block would not balance the flux out of the block exactly. The ratio of flux into and out in block 1 is computed

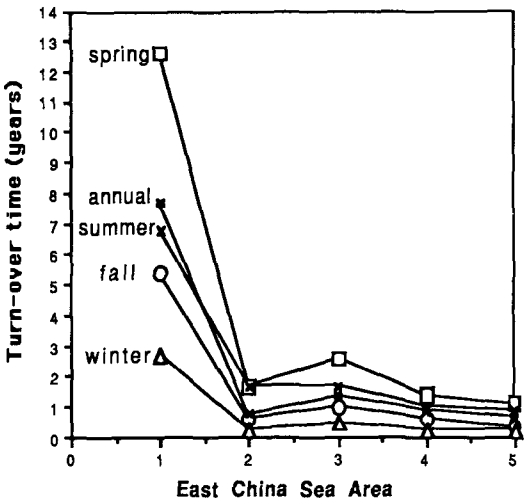

Fig. 10. Turn-over time of the surface layer.

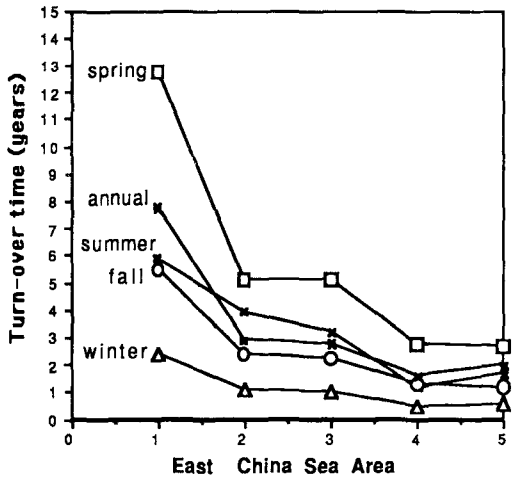

Fig. 11. Turn-over time of the mid-depth layer (or 2D)

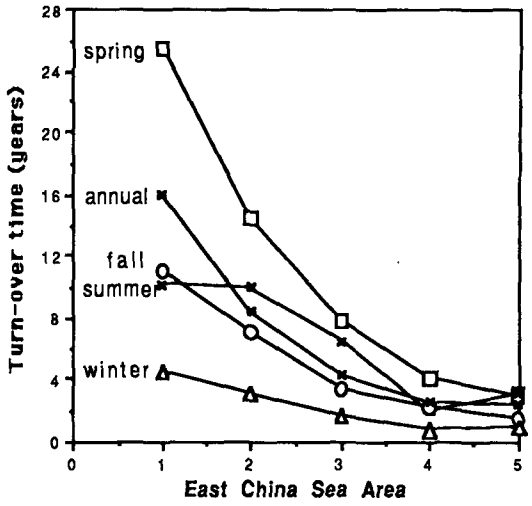

Fig. 12. Turn-over time of the bottom layer.

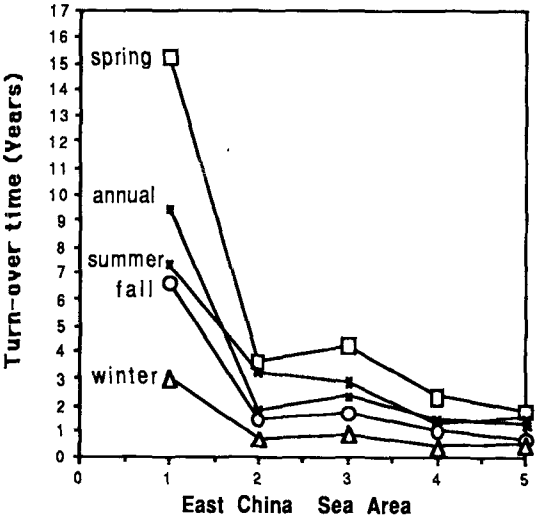

Fig. 13. Turn-over time of the total water depth column (3D).

lager than that in other blocks. Second, the vertical flux may have to be considered in computing the total flux, but this is ignored in present study. Davies(1982) pointed out that, although the vertical velocity is approximately less than one hundredth of the horizontal velocity, the horizontal area of the grid box involved in the flux calculation is large and hence the vertical flux may be appreciable. On the whole, it might be concluded that these two factors have an effect on computing the turn-over time in block 1.

It is evident from Table 2 and Fig. 10, 11, 12 and 13, that the turn-over time for the surface layer is significantly less than for the bottom layer, due to the reduction in current magnitude with depth. Also, T exhibits a strong seasonal dependency, reflecting the seasonal variations in the magnitude of the wind stress, and varies from one region of the East China Sea to another. Considering the turn-over time of the total water depth (3D), it is evident from Figure 10 that for all seasons and annual, block 1 has the largest value. Altough the volume

of block 1 is small, it is apparent from Fig. 3 to 7 that the magnitudes of current are significantly smaller than other regions. Whereas, turn-over time of the total water depth in block 5 has the shorter T except summer period, due to the higer magnitudes of current (Fig. 3 to 7). Since the magnitudes of current in block 4 is higher than block 5 in summer periods, T of block 4 has larger than that of block 5.

5. CONCLUDING REMARKS

This paper has presented a short account of some numerical modeling relating to major features of the East China Sea circulation from season to season. The magnitude and direction of the annual and seasonal meteorologically-induced currents are shown remakable variations in the east china sea continental shelf. Therefore, it is necessary to use a three-dimensional model for studying wind-induced circulation in this area.

The short turn-over time (of the order of days in winter periods) for the surface layer, it is the magnitude of wind stress on a daily, and not a seasonal basis, which will determine how long it takes a pollutant in the surface layer to leave a particular sea region. In present study the vertical flux is not considered in computing of the total flux, but it can be appreciable to calculate the total flux (Davies, 1982). Also, the results of computed turn-over time are presented the importance of the division of sea areas. In future study the verical flux may have to be considered in computing of the total flux and more reasonable division of the East China Sea areas will be necessary.

The concept of turn-over time is considered as a important factor to study pollution problems, such as accident of oil spill and release of radionuclides from radioactive waste repository located in the vicinity of the coastal zone. Especially, the computed turn-over time is provided with input data of ocean box model (Suh *et al.*, 1991) which represents the spatial distribution of radionuclide in the sea area.

ACKNOWLEDGEMENT

This research was funded by CRAY University Grant.

REFERENCES

Bolin, B. and Rodhe, H., 1973. A note on the concepts of age distribution and transit time in natural waters, Tellus, **25**: 58-62.

Choi, B.H., 1980. A tidal model of the Yellow sea and the Eastern China Sea, Korea Ocean Research and Development Institute Repart 80-02.

Choi, B.H., 1982. Note on currents driven by a steady uniform wind stress on the Yellow Sea and the East China Sea, La mer, **20**: 65-74.

Choi, B.H., 1984. Computation of currents driven by a steady uniform wind stress on the East China Sea using a three-dimensional numerical model, The Jour. of the Oceanol. Soc. of Korea, 19, **1**: 36-43.

Choi, B.H., 1985. Observed and computed tidal currents in the East China Sea, Jour. of Oceanol. Soc. of Korea, 20, **1**: 56-73.

Choi, B.H., 1989. A fine-grid three-dimensional M_2 tidal model of the East China Sea, Modeling Marine Systems, Vol.I: 167-185.

Choi, B.H. and Suh, K.S., 1991. Computation of meteorologically-induced circulation on the East China Sea using a three-dimensional numerical model, (submitted to Yellow Sea Research)

Davies, A.M., 1980. On formulating a three-dimensional hydrodynamic sea model with an arbitrary variation of vertical eddy viscosity, Computer Methods in Appl. Mech. and Eng., **22**: 187-211.

Davies, A.M. and Furnes, G.K., 1980. Observed and computed M_2 tidal currents in the North Sea, Jour. of Phys. Oceanogr., **10**: 237-257.

Davies, A.M., 1982. Meteorologically-induced circulation on the North-West Eupropean continental shelf: from a three-dimensional numerical model, Oceanologica Acta, 5, **3**: 269-280.

Han, Y.J. and Lee, S.W., 1981. A new analysis of monthly mean wind stress over the global ocean, Climatic Research Institute, Oregon State Univ., rep. No.26.

Heaps, N.S., 1972. On the numerical solution of the three-dimensional hydrodynamic equations for tide and storm surges, Mem. Soc. R. Sci. Liege, ser., 6, **2**: 143-180.

Japan Meteorological Agency, 1968. Normals of monthly mean sea-level pressure for the northern and southern hemispheres, Forecating Res. Lab., Mete. Res. Inst. Technical Report No.61.

Niino, H. and Emery, K.O, 1961. Sediments of shallow portions of East China and South China Sea, Geol. Soc. Amer. Bull., **72**: 731-762.

Suh, K.S. et al., 1991. Modeling study on nuclide transport in ocean: an ocean compartment model, Jour. of the Korean Nuclear Society, (submitted).

U.S. Naval Oceanographic Office Pub. No.237, 1964. Ocean currents in the vicinity of the Japanese islands and China coast.